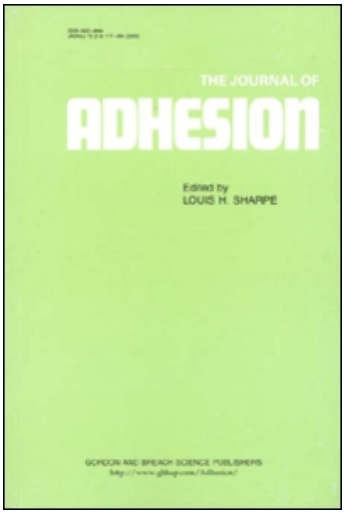

The Journal of Adhesion
Publication details, including instructions for authors and subscription information:
http://www.informaworld.com/smpp/title~content=t713453635

Peel strength of uncrosslinked styrene-butadiene rubber adhered to polyester film

G. R. Hamed[a]; W. Preechatiwong[a]
[a] Polymer Science Department, The University of Akron, Akron, Ohio, USA

Online publication date: 08 September 2010

To cite this Article Hamed, G. R. and Preechatiwong, W.(2003) 'Peel strength of uncrosslinked styrene-butadiene rubber adhered to polyester film', The Journal of Adhesion, 79: 4, 327 — 348
To link to this Article: DOI: 10.1080/00218460309582
URL: http://dx.doi.org/10.1080/00218460309582

The Journal of Adhesion, 79: 327–348, 2003

0021-8464/03 $12.00 +.00
DOI: 10.1080/00218460390148167

Taylor & Francis
Taylor & Francis Group

PEEL STRENGTH OF UNCROSSLINKED STYRENE-BUTADIENE RUBBER ADHERED TO POLYESTER FILM

G. R. Hamed
W. Preechatiwong
Polymer Science Department,
The University of Akron,
Akron, Ohio, USA

Testpieces consisting of a fabric-backed styrene-butadiene rubber (SBR 1502) layer bonded directly to polyethylene terephthalate (PET) film were T-peel tested at various rates, **R**, *and temperatures. Peel energies were superposed to form master-curves using shift factors,* $\mathbf{a_T}$, *in accord with the universal WLF equation. When peeled at intermediate reduced rates,* $\mathbf{Ra_T}$, *failure was cohesive within the SBR 1502, while at sufficiently high or low* $\mathbf{Ra_T}$ *interfacial separation between the rubber and PET occurred. These results markedly contrast with those found by Gent and Petrich using similar testpieces with another type of rubber, SBR 1513. They found cohesive failure at sufficiently low* $\mathbf{Ra_T}$ *and interfacial failure when* $\mathbf{Ra_T}$ *was high. The different behavior of the two elastomers is attributed to stronger interfacial attraction with SBR 1513 and its lower strength. General considerations governing the locus of failure during peel adhesion testing are discussed.*

Keywords: Rubbery peel adhesion; Rate and temperature dependence; Failure loci

INTRODUCTION

Gent and Petrich [1], using the T-peel geometry shown in Figure 1, measured the peel strength at various rates and temperatures of styrene-butadiene rubber (SBR) adhered to polyethylene terephthalate film (PET). Results are shown in Figure 2 for test specimens containing an uncrosslinked SBR layer (Ameripol® 1513, Table 1). Two different loci of failure were observed: "C" denotes cohesive failure within the rubber layer during peeling, while "I" signifies

Received 6 August 2001; in final form 28 August 2002.
Funding for this work was provided by the D'Ianni Research Endowment.
Address correspondence to Gary R. Hamed, Polymer Science Department, The University of Akron, Akron, OH 44325-3909, USA. E-mail: hamed@polymer.uakron.edu

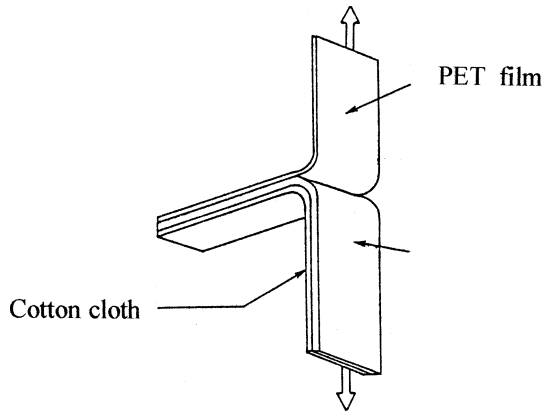

FIGURE 1 T-peel test specimen.

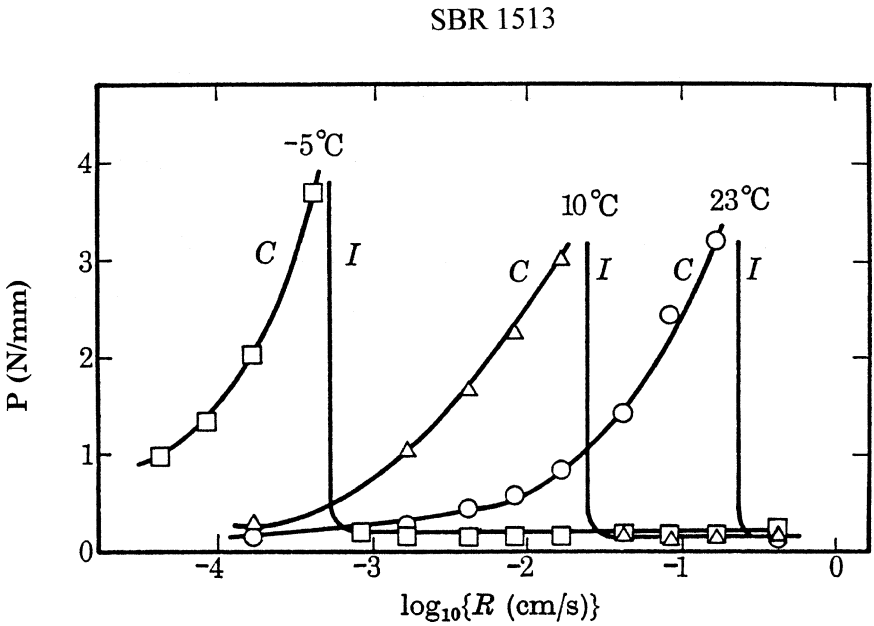

FIGURE 2 Peel strength at various rates and test temperature of SBR 1513 bonded to PET. C and I denote cohesive and interfacial failure modes [1].

interfacial detachment of the layer from the film. Using shift factors, $\mathbf{a_T}$, calculated from the universal WLF equation, the data were shifted horizontally to form a mastercurve (Figure 3). This time-temperature superposability established that the peel strength of a simple,

TABLE 1 Characteristics of Styrene Butadiene Rubbers

	Ameripol® 1513	Plioflex® 1502[c]
% Styrene	40	23.5
$M_n \times 10^{-5}$ g/mol	0.67	1.0
% Gel	0	0
T_g°C (DSC)	−40	−55
Product stain	NST[a]	NST
Emulsifier	FA-RA[b]	FA-RA
ML/1 + 4/100°C	36	52
Coagulation	Alum	Acid or salt acid
Type	Cold emulsion	Cold emulsion

[a] Nonstaining.
[b] Fatty acid−rosin acid.
[c] SBR 1502 from the Goodyear Chemical Co., Akron, Ohio, USA.

amorphous rubber adhering to a rigid substrate depended on the molecular segmental mobility of its chains in the same way as other viscoelastic properties, *e.g.*, creep compliance or stress relaxation modulus. Gent and Petrich also plotted Young's modulus of the rubber (*versus* the appropriate corresponding reduced rate) and the peel mastercurve together (Figure 4). The authors noted that:

1. The transition from cohesive to interfacial failure and the corresponding drop in peel strength is clearly associated with the transition from liquid-like to rubber-like behavior.
2. The second peak in the peel behavior is associated with the transition of the layer from the rubbery to the glassy state.

From these results, it appeared that the transitions in peel adhesion over a broad range of temperature and rates were simply controlled by the viscoelastic properties of the bulk polymer.

The present article demonstrates that the findings of Gent and Petrich are not general for the peeling of uncrosslinked, amorphous rubber. We studied the T-peel behavior (as in Figure 1) of another uncrosslinked SBR (Plioflex® 1502, Table 1) adhered to PET. Attention is focused on: (1) an additional transition, not found by Gent and Petrich, from cohesive to interfacial failure as $\mathbf{Ra_T}$ *decreases* and (2) detailed failure loci during peeling. To understand transitions in the locus of failure during peeling, it is necessary to consider not only the rate/temperature dependence of the strength of the bulk polymer but also that of the interfacial bonds.

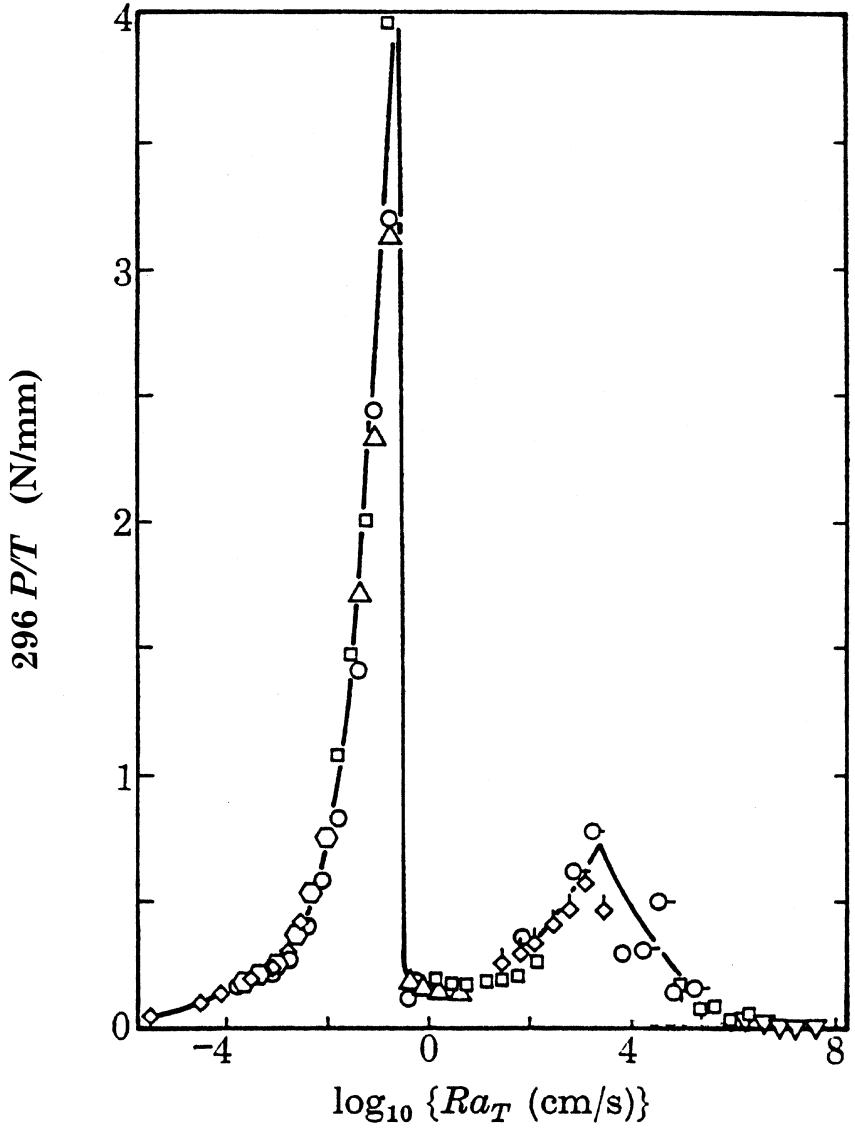

FIGURE 3 Mastercurve produced by WLF shifting of data in Figure 2 [1].

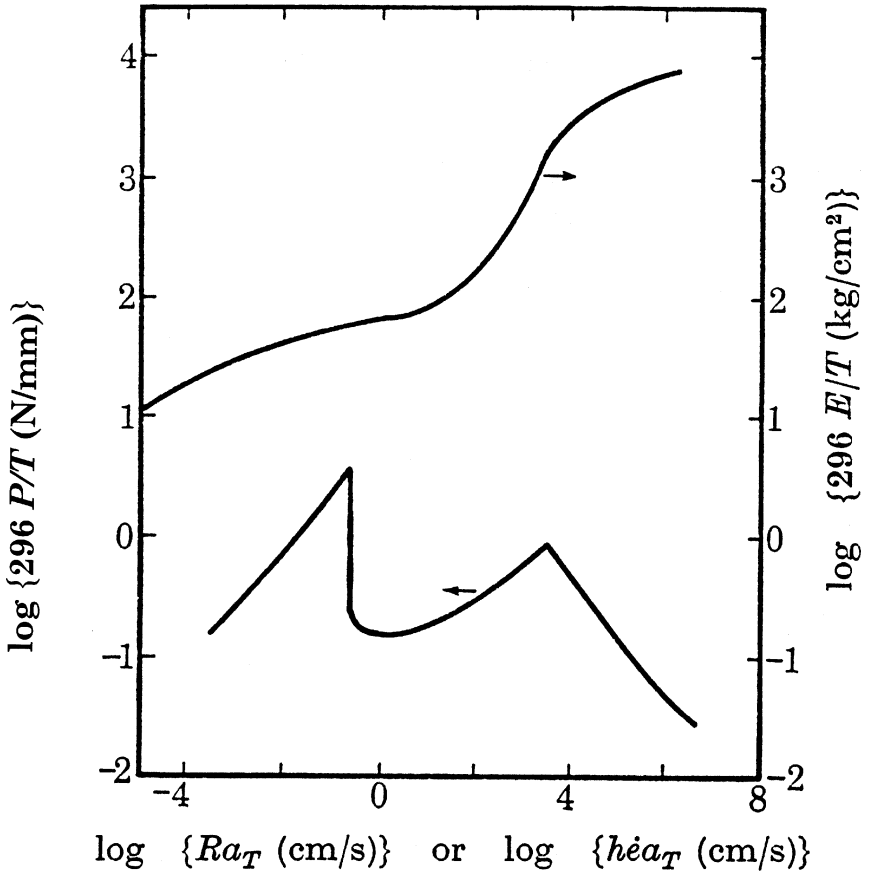

FIGURE 4 Comparison of peel mastercurve for SBR 1513 with its Young's modulus E at corresponding test rates [1].

EXPERIMENTAL

Test plaques were made in a window mold by pressing a layer of SBR 1502 between PET (Dupont Mylar® film, Dupont Co., Wilmington, Delaware, USA) and cotton fabric at 140°C for 20 min. In the laminates, the thicknesses of the cloth, PET, and rubber layer were about 0.6 mm, 76 μm, and 0.9 mm, respectively. T-peel test strips 20 mm wide were cut and pulled apart at various rates and temperatures. Peel energies are given by twice the peel force per unit width. Cohesive fracture (C) was easily determined visually, and the amount of rubber left on peeled PET pieces was determined by weighing them. Interfacial failure (I) was established when no rubber was seen on the

peeled PET, and the contact angle on the film was the same as that on the starting PET ($\theta = 52°$, ethylene glycol).

RESULTS AND DISCUSSION

Figure 5 shows peel energies of testpieces with the SBR 1502. Values determined at various rates, **R**, and temperatures have been shifted

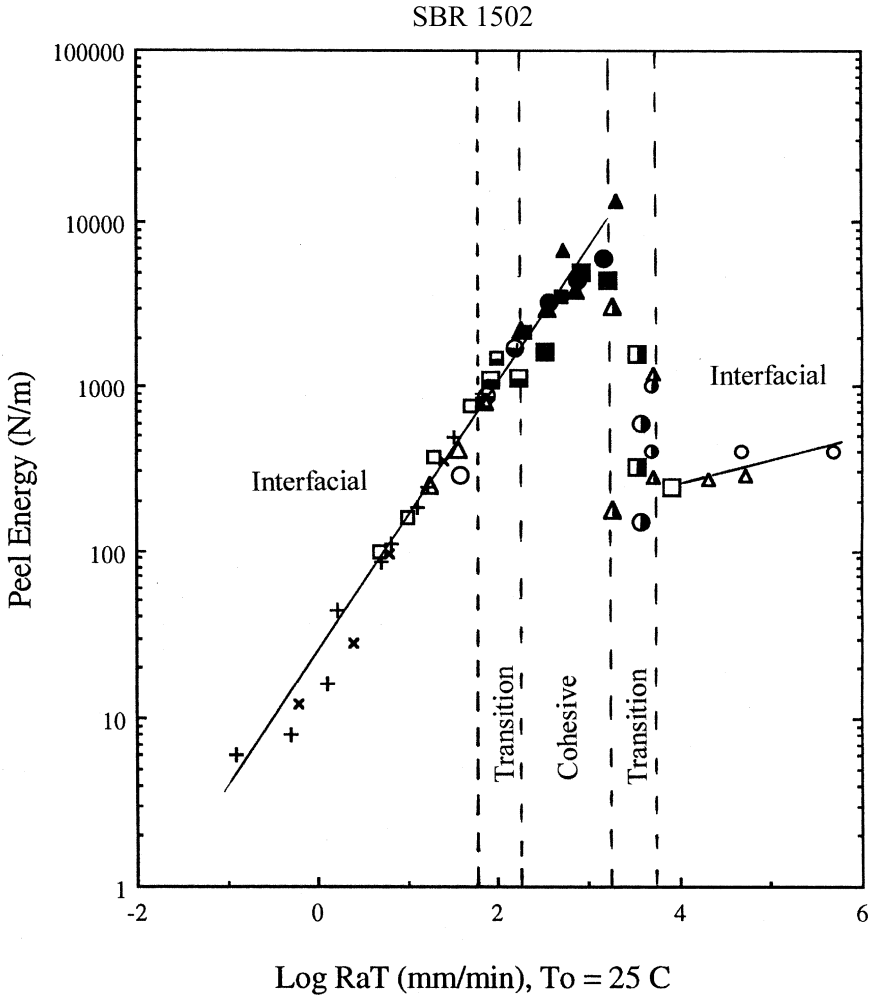

FIGURE 5 Peel adhesion mastercurve for SBR 1502 bonded to PET, constructed using universal WLF shift factors.

horizontally using shift factors calculated from the universal WLF equation with $T_0 = 25°C$. The data superpose to form a mastercurve, which shows a C → I transition with increasing reduced rate and a large abrupt decrease in peel force at a critical log $\mathbf{Ra_T} \approx$ 3.25 mm/min. When failure is cohesive (filled symbols, log $\mathbf{Ra_T} \approx$ 2.25–3.25 mm/min), the peel force is rather steady—with only small, irregular fluctuations. In the (high-rate) transition region (log $\mathbf{Ra_T} \approx 3.25–3.75$ mm/min, right half-filled symbols), two values of peel energy are plotted for each reduced rate, since the peel force oscillates regularly between high initiation and low arrest values (so-called stick-slip). The difference between the "stick" and "slip" peel forces diminishes as rate increases. When log $\mathbf{Ra_T}$ is greater than about 3.75 mm/min, interfacial peeling becomes steady and peel energy increases slowly with increasing peel rate.

Failure Loci

The behavior described in the above paragraph was also found by Gent and Petrich as illustrated in Figure 3 (although Figure 5 lacks a second peak, since rates do not extend to the glassy range). However, unlike their results, another C → I transition is seen in Figure 5 as $\mathbf{Ra_T}$ *decreases*. Beginning at the highest rate where cohesive failure occurs (log $\mathbf{Ra_T} \approx 3.25$ mm/min) and proceeding to lower rates, failure, at first, remains fully cohesive within the SBR, but *the locus of failure shifts closer to the SBR/PET interface*, *i.e.*, the peeled PET film is completely covered with fractured rubber, but less rubber is left on the PET as peel rate decreases.

Figure 6 is an optical micrograph of a PET strip after peeling within the (fully) cohesive failure region. The surface of the rubber left on the PET is rough due to localized yielding and extensional flow of the rubber during fracture. Wisps of rubber formed by drawing and necking of fibrils are apparent. From the weight of pieces of peeled films, the average thickness, **t**, of rubber left on them was determined. The maximum value of **t** was about 0.22 mm. The thickness, **h**, of the entire rubber layer prior to peeling was about 0.9 mm. Thus, about one-fourth of the rubber layer is left on the PET film during cohesive failure near the high-rate transition. The amount of rubber left on the peeled PET decreases with decreasing rate—reaching a thickness of about 0.01 mm when log $\mathbf{Ra_T} \approx 2.25$ mm/min, *i.e.*, just before the low-rate transition.

Figure 7 shows values of **t** for various peel rates and test temperatures. (Data are limited to conditions where failure is fully cohesive, log $\mathbf{Ra_T} \approx 2.25–3.25$ mm/min). The data appear to show time-temperature

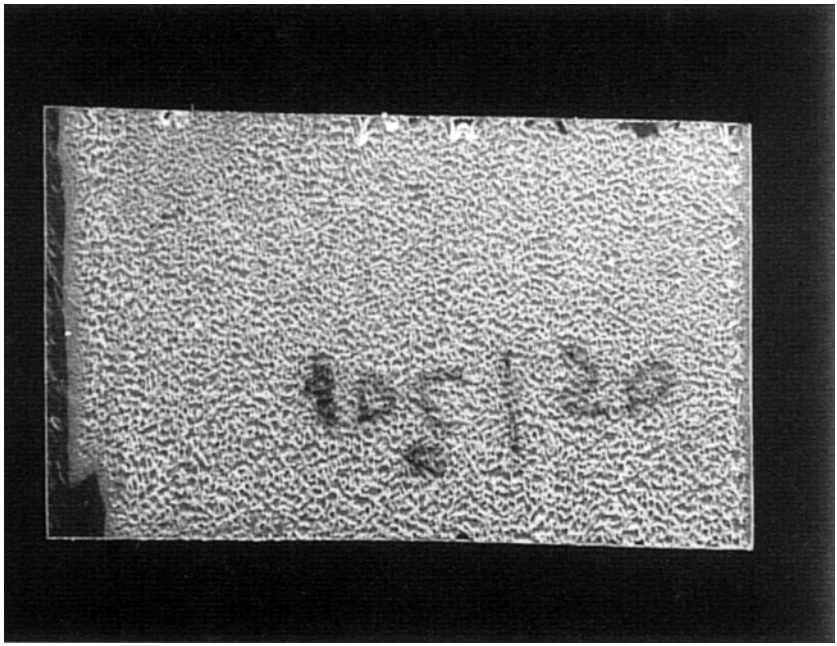

FIGURE 6 Optical micrograph of the surface of a piece of PET film after peeling within the cohesive failure regime for SBR 1502. (The dark image is writing in black ink on the backside of the PET).

equivalence, with a value of **t** at an arbitrary temperature and rate also attainable at some lower temperature and lower rate. Indeed, using shift factors calculated from the universal WLF equation, the data may be superposed to form a mastercurve (Figure 8). High peel strengths within the cohesive failure regime are found at high $\mathbf{Ra_T}$ and they are associated with fracture loci deep into the rubber layer. Because of transitions in failure loci, the data in Figure 8 should not be extrapolated to predict the behavior outside the range given.

With a further reduction in peel rate, a transition (log $\mathbf{Ra_T} \approx 2.25$ mm/min) toward interfacial failure begins, as the failure locus becomes mixed (symbols with their lower part half filled in Figure 5). Peel energies show no discontinuity at this low-rate C $\rightarrow$ I transition. Here, peeled PET films exhibit both interfacial failure regions and random "patches" of rubber torn from the SBR layer (Figure 9). The transition region occurs over about a half decade of $\mathbf{Ra_T}$, and within it the thickness of the rubber patches remains constant at about 0.01 mm. However, the percent of the fracture surface

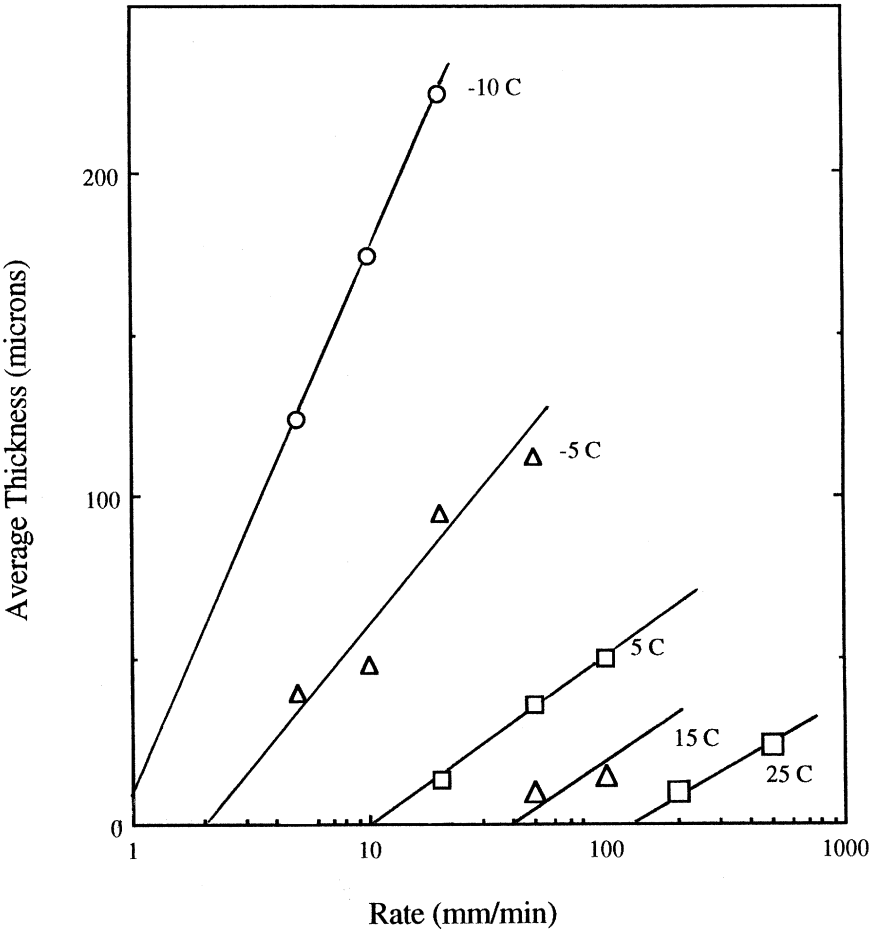

FIGURE 7 Average thickness of SBR 1502 left on peeled PET strips as a function of peel rate and test temperature. Data are for the *fully* cohesive failure regime only.

which is interfacial increases as rate decreases. Cohesive failure not only is localized near the interface but also becomes increasingly localized laterally as peel rate decreases within the transition zone.

Eventually, at sufficiently low peel rates (log $\mathbf{Ra_T} \leq 1.75$ mm/min), failure becomes completely interfacial and remains this way down to the lowest values of $\mathbf{Ra_T}$ tested. The surface of the peeled rubber is quite smooth, even though the peel rates correspond to the elastomer's flow regime. Detachment stresses are so low that the surface region does not undergo plastic flow during peeling.

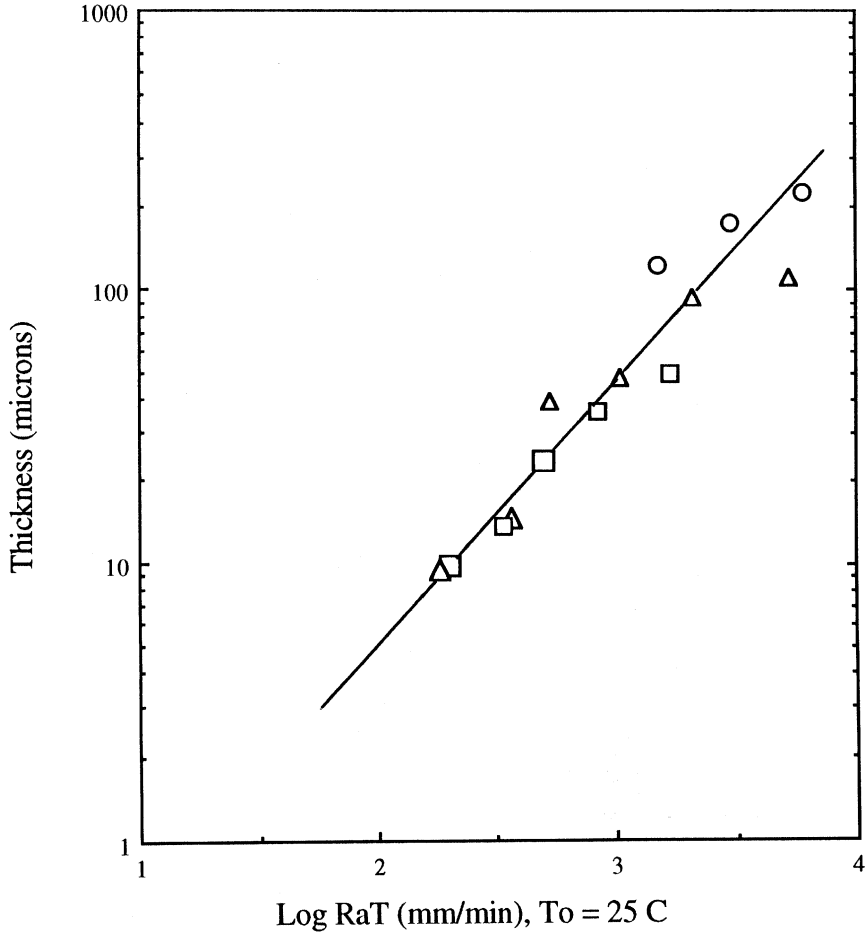

FIGURE 8 Mastercurve produced by WLF shifting of data in Figure 7.

Although both the high-rate and low-rate C/I transitions occur over a range of $\mathbf{Ra_T}$ of about half a decade, the two transitions exhibit quite different characteristics. In the high-rate C/I transition, the peel force oscillates in a regular stick-slip manner. When peeling within this transition zone, failure is completely interfacial, with a characteristic pattern left on the detached rubber after peeling. No rubber is left on the PET, but the rubber surface shows alternating bands (across the width) of rough and smooth regions—corresponding to the stick and slip peel forces, respectively. During stick, the peel force slowly increases to a maximum and the rubber surface distorts enough to

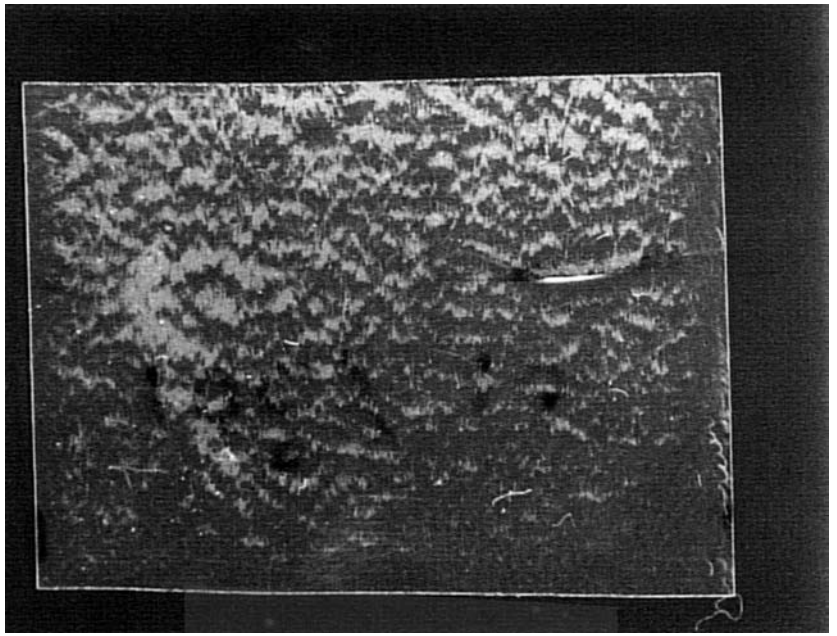

FIGURE 9 Optical micrograph of the surface of a piece of PET film after peeling within the low-rate transition regime for SBR 1502. Light patches are areas of cohesive failure, while failure is interfacial in darker areas.

cause visible roughening, but before the onset of extensive yielding, the peel front jumps forward (slips) leaving a very smooth, shiny surface as the peel force drops to a minimum. The peel force then begins to increase toward the stick portion and the process repeats.

We now turn attention to a direct comparison of the peel results in this work with those of Gent and Petrich and attempt to explain the differences.

SBR 1513 Compared with SBR 1502

In Figure 10, the peel mastercurves for the two types of SBR adhered to PET are plotted together. Peel energies for each rubber have been reduced to 25°C using shift factors determined from the universal WLF equation with corresponding glass transition temperatures. The data "points" are identical to those plotted in Figure 5, while the lines labeled "G-P PET" are the same ones fitted to the data in Figure 3. When log $\mathbf{Ra_T}$ is greater than about 2.25 mm/min, the response with SBR 1502 is like that with SBR 1513. Testpieces with either rubber fail

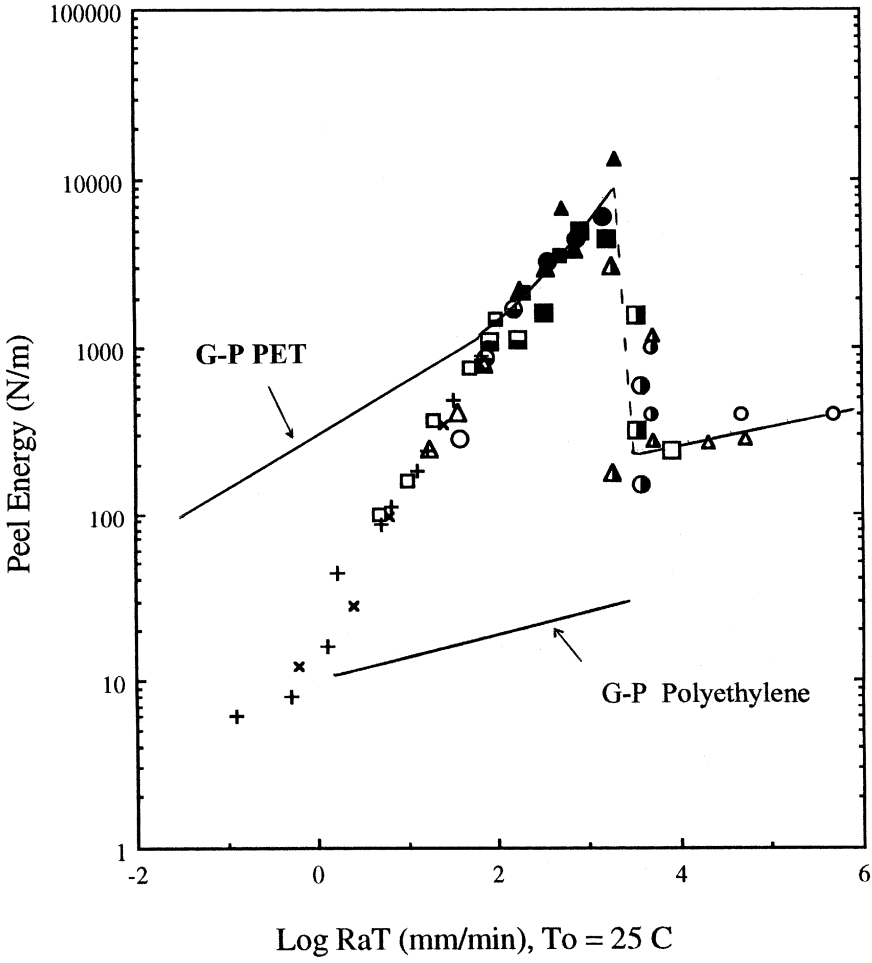

FIGURE 10 Comparison of peel mastercurves for SBR 1513 and SBR 1502. The lines drawn are Gent-Petrich results for SBR 1513 bonded to PET [1] and for SBR 1513 bonded to untreated polyethylene [2]. The data points are for SBR 1502 bonded to PET and are identical to those plotted in Figure 5.

cohesively at similar peel forces, then failure transitions discontinuously to interfacial at a critical rate (log $\mathbf{Ra_T} \approx 3.25$ mm/min). However, the low-rate behavior is strikingly different. While failure remains cohesive with SBR 1513, specimens with SBR 1502 transition to interfacial failure and exhibit much lower peel strength.

SBR 1502 and SBR 1513 are characterized in Table 1. Both are gel-free, cold-emulsion rubbers. The higher styrene content of SBR 1513 is

expected to result in stronger interfacial attraction to PET compared with SBR 1502/PET bonding. Additionally, SBR 1513, because of its lower molecular weight, has a lower yield stress than SBR 1502. Apparently, these factors cause the SBR 1513 to have an increased tendency toward cohesive failure compared with SBR 1502.

Gent and Petrich [1] reported on the peel adhesion of SBR 1513 bonded to various substrates including PET (already discussed), cellophane, polystyrene, and transcrystalline polyethylene. In all these cases, failure was cohesive at sufficiently low (reduced) rates and transitioned abruptly to interfacial at some critical rate. The critical rate was highest for the polystyrene (strongest adhesion) and lowest for the transcrystalline polyethylene (weakest adhesion). Thus, failure locus depends not only on the viscoelasticity of the rubber layer but also on its intrinsic adhesion to the substrate. Indeed, if intrinsic adhesion is low enough, the locus of failure may be interfacial at all rates and temperatures, even for a soft, hydrocarbon rubber like SBR 1513. Such behavior is shown [2] (Figure 10, "G-P polyethylene") when SBR 1513/untreated polyethylene specimens are peeled apart. The bonding between SBR 1513 and untreated polyethylene is so low that failure is interfacial even when rates of peeling correspond to the flow regime of the rubber.

Figure 10 shows that the peel results for SBR 1502/PET lie between those for SBR 1513/PET and SBR 1513/untreated polyethylene. This suggests that the intrinsic adhesion of SBR 1502 to PET may be intermediate as well, giving rise to the new behavior. The role of interfacial interactions on the viscoelastic response of adhesive joints is considered next.

INTERFACIAL CONSIDERATIONS

Consider an uncrosslinked, hydrocarbon rubber bonded to a substrate. Chains in the bulk of the rubber are highly entangled and interact by weak van der Waals forces; chains are in rapid segmental motion. The interaction of a particular bulk chain with neighboring chains may be characterized by the product of the number, $\mathbf{n_b}$, of intermolecular (physical) bonds times the interaction energy, $\varepsilon_\mathbf{b}$, per bond. Though $\varepsilon_\mathbf{b}$ is small for an uncrosslinked hydrocarbon rubber, it, nonetheless, is solid-like because $\mathbf{n_b}$ and hence the product $\mathbf{n_b}\varepsilon_\mathbf{b}$, is large. In a similar way, the total interfacial interaction between the rubber and substrate may be characterized by $\varepsilon_\mathbf{i}\mathbf{n}_\mathrm{i}$, where ε_i is the specific interfacial interaction energy and $\mathbf{n_i}$ is the number of these formed at the interface. In principle, $\varepsilon_\mathbf{i}$ can range from the weakest possible physical bonds to strong chemical linkages. The magnitude of $\mathbf{n_i}$ depends on the

extent of interpenetration between the rubber and substrate. If adhesion is limited to adsorption at surface sites, then $\mathbf{n_i}$ will be relatively small, while $\mathbf{n_i}$ increases as elastomer/substrate interdiffusion increases.

SBR and PET are thermodynamically incompatible and develop a sharp interface when contacted. Nonetheless, under some test conditions the (highly entangled) SBR chains disentangle and flow apart (*i.e.*, fail cohesively), rather than simply detaching from the PET. In order to explain this behavior we adopt the approach taken by Gent and Petrich. They considered the effect of (reduced) test rate on the stress-strain response of uncrosslinked SBR 1513. When deformed slowly, this material exhibited a yield point, then drew down in a plastic flow process. Under this circumstance, the stress necessary to detach the rubber from the PET exceeded the yield stress of the rubber, and fracture occurred by cohesive failure. However, at sufficiently high deformation rates the rubber exhibited strain-hardening, and its tensile strength exceeded the interfacial strength. Now the detaching rubber deformed elastically and failure became interfacial.

We now propose four general cases for the peel adhesion behavior of uncrosslinked rubber. The locus of failure at sufficiently low $\mathbf{Ra_T}$ ("equilibrium" conditions) depends on the relative values of bulk and interfacial interaction energies, while the locus with increasing $\mathbf{Ra_T}$ depends on the change in the fracture resistance of interfacial and bulk segments under "nonequilibrium," viscoelastic conditions.

Case 1: Interfacial

When the total interfacial interaction energy is much less than the energy causing entangled chains to cohere, failure is interfacial over the whole range of $\mathbf{Ra_T}$. The situation is depicted schematically in Figure 11, where stress-strain curves for the rubber are shown for low (L), medium (M), and high (H) rates of deformation. Also shown are (hypothetical) detachment stresses, $\boldsymbol{\sigma}$, which are less than the cohesive (or yield) strength, for all rates of deformation. This is thought to be the situation for SBR 1513 bonded to untreated polyethylene. Interaction of uncrosslinked rubber chains on the surface of a solid substrate may or may not reduce chain mobility compared with that in the bulk. This depends on the strength and number of (adsorptive) bonds formed. For SBR/PE the interface is sharp (low $\mathbf{n_i}$) and specific interactions are weak (low $\boldsymbol{\varepsilon_i}$), probably weaker than $\boldsymbol{\varepsilon_b}$. Rubber chain segments at the interface are thought to have increased mobility compared with bulk chains and hence detachment occurs readily.

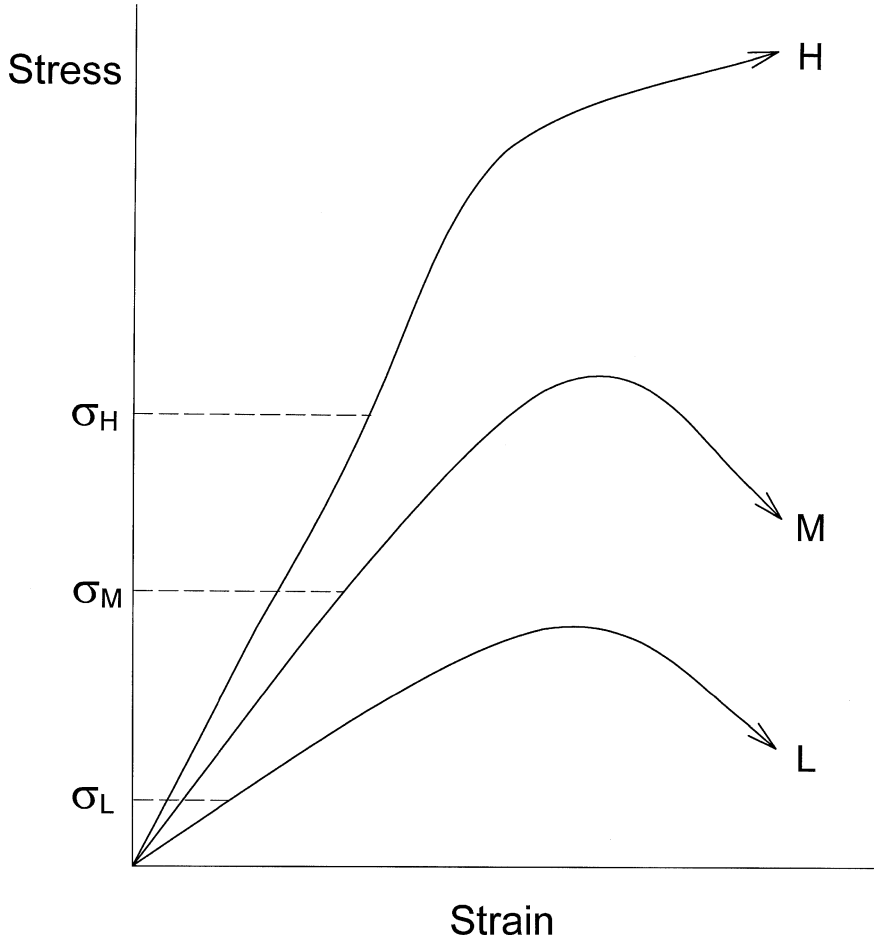

FIGURE 11 Schematic for Case 1 showing stress-strain curves of an elastomer and detachment stresses for various (reduced) test rates. L, M, and H denote low, medium, and high test rates, respectively. Failure is interfacial at all test rates.

For instances of rubber adsorption onto a solid substrate where $\varepsilon_i \approx \varepsilon_b$ and chain segmental mobility at the interface is like that in the bulk, it is expected that simple detachment of a lesser number of adsorbed segments would occur rather than bulk disentanglement, which requires the disruption of a greater number of interchain interactions. Even when ε_i somewhat exceeds ε_b and chain segmental mobility at the interface is somewhat less than that in the bulk, failure still may be interfacial at all $\mathbf{Ra_T}$ if (physical) bonding sites are sparse.

However, with increased ε_i and enough reduction in the mobility of adsorbed chain segments, the locus of failure may change as $\mathbf{Ra_T}$ is increased, as discussed next.

Case 2: Interfacial-to-Cohesive-to-Interfacial

For a given bulk rubber, the interfacial interaction energy somewhat exceeds that for Case 1; peeling transitions from $I \xrightarrow{\text{steady}} C \xrightarrow[\text{slip}]{\text{stick-}} I$ (ICI) as $\mathbf{Ra_T}$ increases. This behavior is shown by SBR 1502/PET. Figure 12

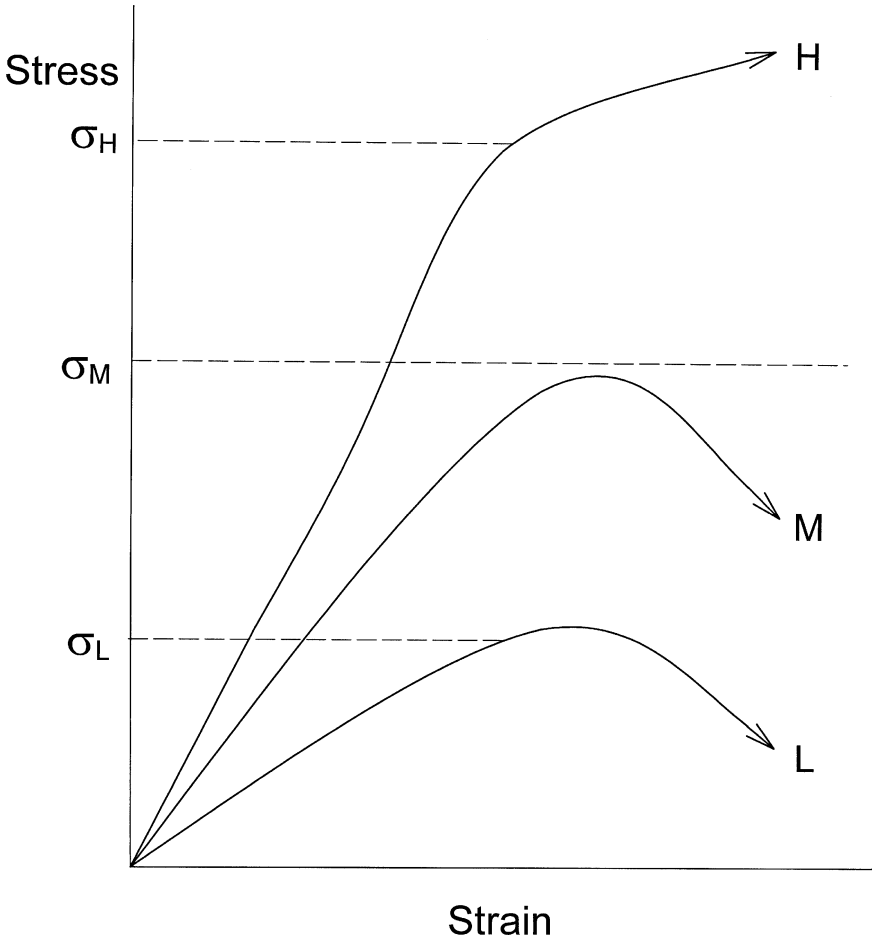

FIGURE 12 As in Figure 11, but for Case 2. Failure transitions from interfacial-to-cohesive-to-interfacial with increasing test rate.

depicts stress-strain curves and corresponding detachment stresses. At low $\mathbf{Ra_T}$, the detachment stress, $\boldsymbol{\sigma_L}$, is less than the bulk (or yield) strength and failure is interfacial. However, at intermediate rates failure becomes cohesive, as $\boldsymbol{\sigma_M}$ now exceeds the rubber's strength. At the highest rates, failure returns to the interface, as elastically effective entanglement couplings provide substantial resistance to bulk fracture.

The yield and cohesive strengths of uncrosslinked rubber depend on chain segmental mobility and the state of chain entanglement. These, of course, reflect the rubber's (low) T_g and (high) molecular weight—for SBR 1502 about -55°C and 10^5 g/mole ($\bar{\mathbf{M}}_\mathbf{n}$), respectively. On the other hand, the detachment strength depends on the mobility of chain segments that have adsorbed and the number of adsorption sites. There are no entanglements across the interface to bolster strength, but interaction with the hard PET slows chain segmental mobility and hence raises T_g of these segments. For this to occur, the interaction energy with the substrate ($\boldsymbol{\varepsilon_i}$) exceeds that among bulk chain segments ($\boldsymbol{\varepsilon_b}$). Nonetheless, failure is interfacial at low $\mathbf{Ra_T}$, because the total interaction energy of the hindered, interfacial segments is still less than the energy required to cause disentanglement of bulk chains. However, the detachment strength does not change in the same way with increasing $\mathbf{Ra_T}$ as do the yield, $\boldsymbol{\sigma_y}$, and cohesive, $\boldsymbol{\sigma_c}$, strengths. Though the interface is sharp, a factor detrimental to strength, the resistance to "pull-off" of adsorbed chain segments increases more quickly with increasing $\mathbf{Ra_T}$ than does $\boldsymbol{\sigma_y}$ or $\boldsymbol{\sigma_c}$. Effectively, the rate response of "partially vitrified" interfacial segments is shifted toward the transition (rubber-to-glass) region of the viscoelastic spectrum, where strength increases relatively rapidly with rate. Failure now occurs by cohesive fracture. At still higher $\mathbf{Ra_T}$, failure returns to the interface as entanglements become elastically effective and the rubber-to-glass transition regime of the bulk rubber is approached.

Case 3: Cohesive-to-Interfacial

With enough increase in interfacial interaction energy relative to the bulk value, peeling transitions from C $\xrightarrow[\text{slip}]{\text{stick-}}$ I with increasing $\mathbf{Ra_T}$. This behavior is shown for SBR 1513/PET bonding and depicted in Figure 13. Though the interface is sharp, chain segments at the interface are now sufficiently "fixed" that their resistance to detachment exceeds the stress necessary for chain disentanglement at low $\mathbf{Ra_T}$. Compared

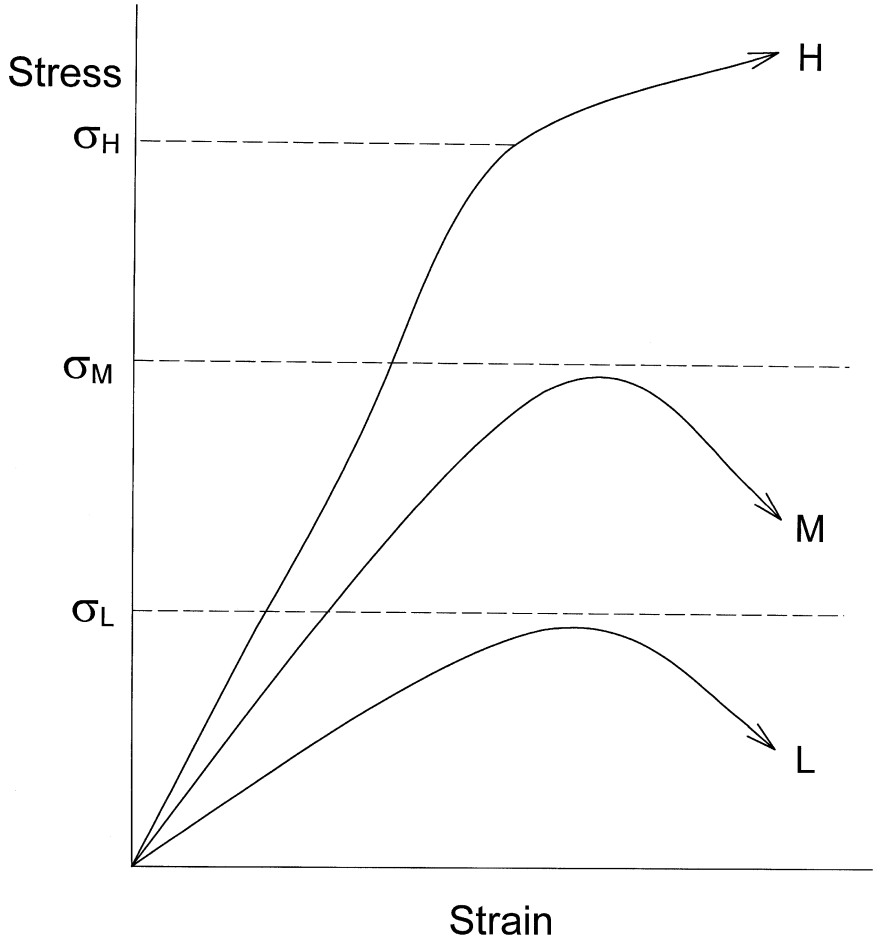

FIGURE 13 As in Figure 11, but for Case 3. Failure transitions from cohesive-to-interfacial with increasing test rate.

with SBR 1502, SBR 1513 has increased interaction with PET (higher ε_i) and less bulk chain entanglement (lower $\mathbf{n_b}$).

Though the resistance to separation of SBR 1513/PET and SBR 1502/PET bonds can increase with increased $\mathbf{Ra_T}$, these bonds, unlike the bulk, do not contain entanglements that become particularly strong at a certain rate regime. In short, the bulk is "polymeric" while the interface is not. At high $\mathbf{Ra_T}$, due to the substantial rise in the elastic behavior (and strength) of the bulk, failure occurs at the ("monomeric") interface.

Case 4: Cohesive

If interfacial bond energies were high enough, it is expected that failure would be cohesive over the whole viscoelastic range (Figure 14). Now, even at the highest $\mathbf{Ra_T}$, the interfacial detachment stress exceeds bulk strength. Though not demonstrated experimentally in this article, Case 4 is expected when there is strong chemical bonding at the interface and for instances of deep interpenetration between the rubber and substrate.

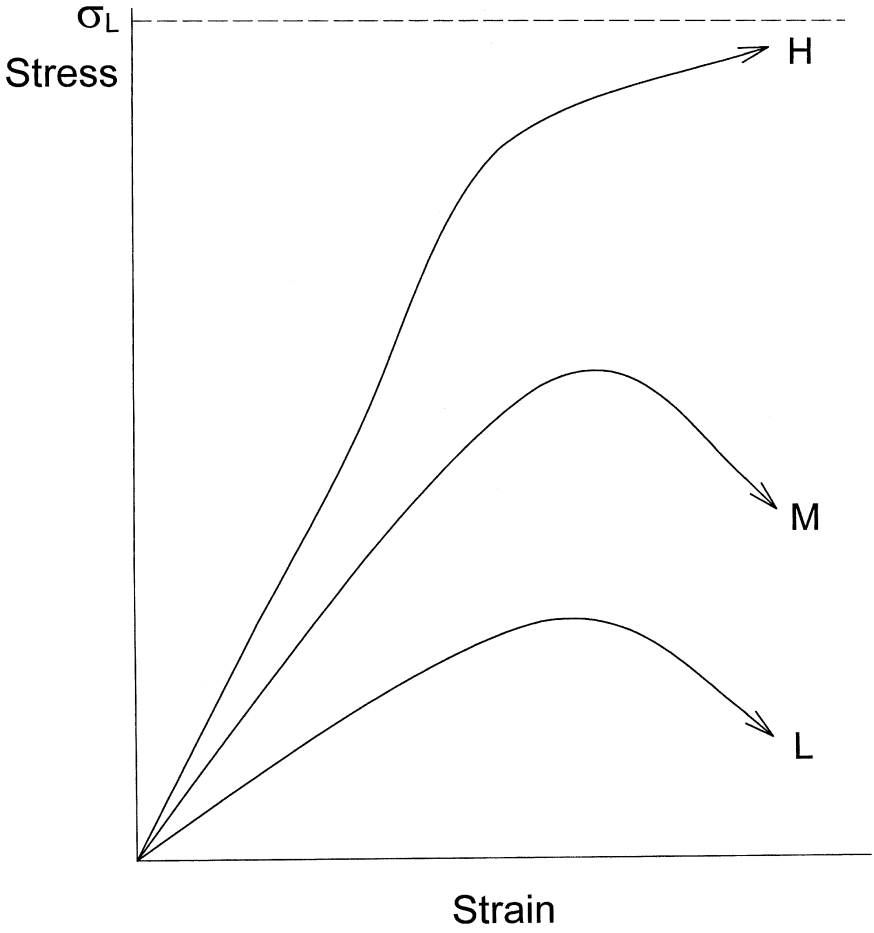

FIGURE 14 As in Figure 11, but for Case 4. Failure is cohesive at all test rates.

CONCLUSION

When a soft, uncrosslinked rubber layer and a hard substrate are peeled apart at various rates and temperatures, the locus of failure depends on the rubber's yield strength, σ_y, or cohesive strength, σ_c, whichever is greater, compared with the interfacial stress, σ_i, required to detach the layer from the substrate. In general, these stresses do not depend on rate/temperature in the same way. We infer that a situation like that shown in Figure 15 occurs for the SBR/PET joints. Figure 15 is a schematic showing the greater of the cohesive or yield strengths (solid lines) of SBR 1502 and SBR 1513 as a function of $\mathbf{Ra_T}$.

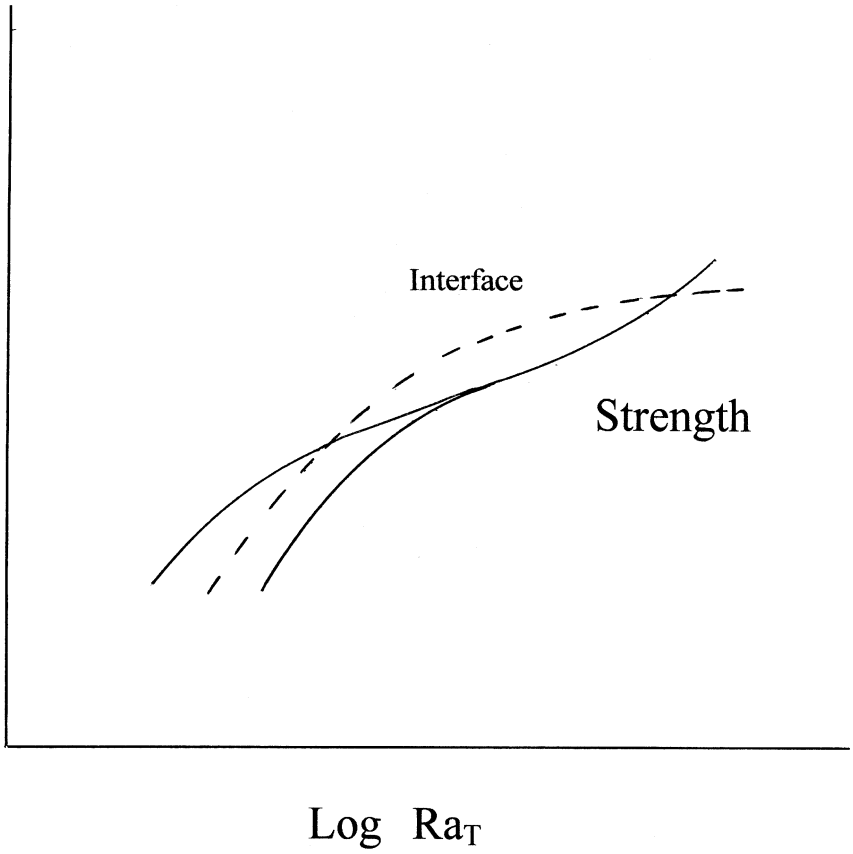

FIGURE 15 Schematic diagram showing, as the solid lines, the greater of the yield strength or the cohesive strength of SBR 1502 and SBR 1513 at various $\mathbf{Ra_T}$. The dotted line is the interfacial detachment stress.

Also shown, as the dotted line, are hypothetical interfacial detachment strengths, drawn in a way that is consistent with the behavior shown in Figure 10. At low rate, ($\boldsymbol{\sigma_c}$ or $\boldsymbol{\sigma_y}$) > $\boldsymbol{\sigma_i}$ for SBR 1502 and failure is interfacial, while for SBR 1513 ($\boldsymbol{\sigma_c}$ or $\boldsymbol{\sigma_y}$) < $\boldsymbol{\sigma_i}$ and cohesive failure occurs. At intermediate rate, $\boldsymbol{\sigma_i}$ becomes greater than ($\boldsymbol{\sigma_c}$ or $\boldsymbol{\sigma_y}$) for the SBR 1502 and failure transitions to cohesive. At high rate, ($\boldsymbol{\sigma_c}$ or $\boldsymbol{\sigma_y}$) > $\boldsymbol{\sigma_i}$ for both elastomers, and failure is interfacial.

Finally, we note that the ICI transition behavior shown for SBR 1502/PET also has been found previously in peel adhesion studies [3]. In Chung and Hamed [3], layers of uncrosslinked butyl rubber and uncrosslinked nitrile rubber were contacted to attain equilibrium bonding, and then joints were peeled apart at various rates and temperatures. Peel mastercurves were generated and ICI transition behavior, like that of SBR 1502/PET, was found with increasing $\mathbf{Ra_T}$. Furthermore, again like SBR 1502/PET, within the low-rate transition regime cohesive failure (of the nitrile rubber) occurred nearer to the interface as $\mathbf{Ra_T}$ was decreased—before failure eventually became completely interfacial.

The peel autohesion (self-adhesion) of various uncrosslinked rubbers also has been shown to exhibit ICI behavior with increasing $\mathbf{Ra_T}$ [4–7]. In autohesion, the specific interaction energy responsible for bonding is the same as that causing cohesion, *i.e.*, $\boldsymbol{\varepsilon_i} = \boldsymbol{\varepsilon_b}$, but $\mathbf{n_i}$ is less than $\mathbf{n_b}$ by an amount that diminishes, as chains interpenetrate, with increasing contact time. After a *short contact time* of 1.5 min, the peel autohesion of SBR 1502 exhibited ICI transitioning with increased $\mathbf{Ra_T}$ [7]. Likewise, the autohesion of a similar, but somewhat lower molecular weight SBR (SBR 146, ML/1 + 4/100°C = 40) also showed this behavior *after brief contact* (1–15 min) [4].

In each of the systems (SBR/PET, butyl/nitrile, SBR/SBR) that have shown ICI behavior, the high rate C → I transition occurred in a "shocky," stick-slip manner. This seems to be associated with a rather weak interface between the contacting materials, either because of poor thermodynamic compatibility (SBR/PET, butyl/nitrile) or because of incomplete bonding (SBR/SBR, brief contact). At longer self-contact time (180 min) for SBR 146, when there is more extensive bonding but still not complete interdiffusion, the high rate, stick-slip C → I transition disappeared. When bonding involves highly entangled chains, stick-slip peeling does not happen, even when peel rates correspond to the rubber's flow-to-entanglement plateau regime. This is another demonstration that the peel response of a rubber is not only dependent on its bulk viscoelastic behavior. With longer contact, autohesion simply shows an I → C transition with increasing $\mathbf{Ra_T}$ [5]. This demonstrates that the peeling of a joint

containing an uncrosslinked rubber is expected to fail interfacially at low rates (even if the rate is within the rubber's flow regime) when significant interpenetration is absent and specific interactions with the substrate cause chain mobility to be like that in bulk. This is thought to be the situation when two incompatible, uncrosslinked rubbers adhere (*e.g.*, butyl/nitrile joint).

REFERENCES

[1] Gent, A. N. and Petrich, R. P., *Proc. Roy. Soc. A*, **310**, 433–448 (1969).
[2] Petrich, R. P., *Adhesion of Elastomers*, Ph.D. Dissertation, University of Akron, Ohio (1968).
[3] Chung, M. H. and Hamed, G. R., *Rubber Chem. Technol*., **62**, 367–385 (1989).
[4] Hamed, G. R. and Shieh, C.-H., *J. Polym. Sci., Physics Ed*., **21**, 1415–1425 (1983).
[5] Hamed, G. R. and Shieh, C.-H., *Rubber Chem. Technol*., **58**, 1038–1044 (1985).
[6] Hamed, G. R. and Shieh, C.-H., *Rubber Chem. Technol*, **59**, 883–895 (1986).
[7] Hamed, G. R. and Wu, P., *Rubber Chem. Technol*., **68**, 248–258 (1995).